Modeling and Performance Evaluation of Three Power Generation and Refrigeration Energy Recovery Systems from Thermal Loss of a Diesel Engine in Different Driving Conditions

H. Golchoobian, M. H. Taheri, S. Saedodin, A. Sarafraz

Abstract—This paper investigates the possibility of using three systems of organic Rankine auxiliary power generation, ejector refrigeration and absorption to recover energy from a diesel car. The analysis is done for both urban and suburban driving modes that vary from 60 to 120 km/h. Various refrigerants have also been used for organic Rankine and Ejector refrigeration cycles. The capacity was evaluated by Organic Rankine Cycle (ORC) system in both urban and suburban conditions for cyclopentane and ammonia as refrigerants. Also, for these two driving plans, produced cooling by absorption refrigeration system under variable ambient temperature conditions and in ejector refrigeration system for R123, R134a and R141b refrigerants were investigated.

Keywords—Absorption system, diesel engine, ejector refrigeration, energy recovery, organic Rankine cycle.

I. INTRODUCTION

ENERGY recovery in energy systems has always been of interest to researchers in order to improve various energy, exergy and economic parameters and in general to improve system performance.

In 2000, a combined cycle of power and refrigeration was presented by Xu et al. [1], and further research by Hassan et al. [2] in 2002, Tamm et al. [3] in 2004, Vidal et al. [4] in 2006, Vijayaraghavan and Goswami [5] in 2006, Martin and Goswami [6] in 2006, Sadr Agali and Goswami [7] in 2007 have been done. In 2006, Zheng et al. [8] presented a combined cycle of power and refrigeration based on the Kalina cycle. The flash of the Kalina cycle tank was replaced by a rectifier which further increased the concentration of the water-ammonia vapor refrigeration cycle. A condenser and an evaporator were inserted between the second absorber and the adsorbent. In 2007, Liu and Zhang [9] introduced a new water-ammonia cycle for the power and refrigeration cogeneration system. The difference of the system presented by them was with the previous variants in a new separation/

adsorption unit. In 2007, Zhang and Lever [10] also introduced a new water-ammonia system for the power and refrigeration cogeneration system. In this system, a water-ammonia Rankine cycle and an ammonia refrigeration cycle are connected in parallel by adsorbents, separators and heat transfer equipment. Zhang and Lever [11] also introduced several hybrid power and refrigeration systems with water-ammonia operating fluid, and provided solutions for how to link power and refrigeration co-generation systems with the aim of enhancing energy and exergy efficiency. In 2008, Wang et al. [12] introduced a power and refrigeration cogeneration cycle that combined Rankine and absorption refrigeration cycles. Subsequently, much research has been done on cogeneration and cooling cycles, most of them combining Rankine or Kalina with absorption cycles, and fewer studies on the combination of Rankin and Ejector refrigeration cycles. The ejector refrigeration cycle has been studied for many years [13]-[18]. Despite its low efficiency, it has important advantages such as fewer moving parts, simplicity of design, and low installation and operating costs. The Ejector Refrigeration Cycle can also use different operating fluids.

The use of heat energy directly to trigger the ejector refrigeration cycle rather than the electrical energy in other cycles has made this cycle a viable option for use in co-generation systems. The use of ejector refrigeration in cogeneration systems as well as the supply of solar energy needed by the system was developed by Golchoobian et al. [19], [20].

Yue and Wang [21] have proposed a vehicle energy delivery system based on heat dissipation of the engine using ORC to meet the vehicle energy requirement of each season. Based on the conventional vehicle engine, the energy supply system of the vehicles was analyzed based on the waste energy recovery. Simulation results show that by reducing the logarithmic mean temperature difference in the first evaporator, decreasing ambient temperature and increasing vehicle speed are three effective ways to increase turbine output power and fuel saving rate. In winter, the highest fuel saving rate is achieved and the power and heat required by vehicles are provided. In the spring and fall, more fuel can be saved and the power required by the vehicle is provided. In summer, the minimum fuel savings and thermal efficiency of the ORC are achieved. Under these conditions, the highest

H. Golchoobian is with the Faculty of Mechanical Engineering, Semnan University, Semnan, Iran and ChatrEnergy Research & Development Company, Tehran, Iran (corresponding author, e-mail: h.golchoobian@gmail.com).

M. H. Taheri and A. Sarafraz are with ChatrEnergy Research & Development Company, Tehran, Iran (e-mail: hasan.taheri@gmail.com, sarafraz.d@gmail.com).

S. Saedodin is with the Faculty of Mechanical Engineering, Semnan University, Semnan, Iran (e-mail: s_sadodin@semnan.ac.ir).

turbine output power and fuel saving rate are 14.7 kW and 0.23, respectively.

Herawan et al. [22] have evaluated the thermal energy of the combustion engine exhaust gas using an artificial neural network. The Sedan's internal combustion engine is selected as the case study model. Performance recovery has been achieved by recovering the heat energy of the engine exhaust gases. It was observed that the amount of energy dissipated is about 23 kW. Mashhadi et al. [23] studied the low temperature Rankine cycle to increase the heat recovery of the internal combustion engine cooling system. The overall dissipative heat of the engine coolant fluid is absorbed by the low temperature Rankine cycle through the operating fluid flow at low discharge. This not only increases the efficiency and power of the system, but also reduces the size of the recovery system. The system is capable of recovering 57% of the energy contained in the cooling fluid. In addition, the conventional radiator system in the cooling system will be eliminated this way. By thermodynamic analysis of 19 different operating fluids, the adaptive conditions between the low temperature Rankine cycle with the engine cooling system and the fluid properties were evaluated. The overall conclusion was that ammonia has a higher potential with the proposed system. Temperature sensitivity analysis was performed for the low temperature Rankine cycle with ammonia as a hot fluid and it was found that changing the ambient temperature had little effect on the cooling fluid temperature. Finally, the results obtained from the low-temperature Rankine cycle were compared with the results of the other six tasks and it was shown that the amount of energy recovered from the proposed system was greater than that of the other six studies.

Patel et al. [24] proposed modeling and thermoeconomic optimization of an ORC and compression-absorption refrigeration hybrid system for thermal loss utilization. The ORC with the dry organic operating fluid is used as the power generation cycle to be used as the input of the steam compression refrigeration system. In addition, high temperature organic fluid is used at the expander output to provide the thermal requirement of the vapor absorption refrigeration system. The proposed system has a low temperature cooling efficiency. However, its initial cost and complexity make it a practical constraint. The energy efficiency of this system is only 22.3% and 79% for cooling and cogeneration modes (cooling and heating), respectively. Excess heat available apart from the heat energy required by the steam absorption system is obtained through the co-generation heat process. The return period is 5.26 and 4.22 years, respectively.

Yue et al. [25] proposed an automated energy auxiliary system through the heat recovery of ORC subsystems. Based on the actual performance data of the vehicle engine at different loads, the overall thermal and economic performance of the proposed system was evaluated by comparing it with conventional systems considering the effects of ambient temperature, operating fluid selection and turbine inlet temperature in different seasons. The results of the analysis showed that the proposed system exhibits better thermal and economic performance than conventional systems. As the season changes, the proposed system performs better in winter, then in autumn, spring, and finally in summer. Also, Cyclopentane is the best operating fluid for this proposed system.

Salek et al. [26] coupled an absorption and Rankine cooling cycle with a diesel engine to recover the energy of the exhaust gases. The innovation is the use of the ammonia absorption refrigeration cycle under the Rankine cycle coupled to a diesel engine to generate more power. The subsystem converts the heat output of the engine output into cooling and mechanical energy. The energy transfer process is carried out by two shell tube heat exchangers. According to the results, the energy recovered varies with the amount of diesel engine load. For the specific load values investigated in this study, the use of two heat exchangers causes a 0.5% reduction in the mechanical power of the motor. However, the energy recovered is 10% of mechanical power. Fu et al. [27] evaluated the efficiency of gasoline engine energy use and estimated dissipative heat energy recovery, energy distribution, and dissipative heat energy characteristics of gasoline engines using energy and exergy analysis. During the research process, the engine energy balance tests were carried out under specified conditions and the parameters needed to calculate the energy balance and exergy were measured. Accordingly, the energy recovery capability and overall exergy efficiency of a gasoline engine have been studied using the exergy analysis method. The results show that at low engine speed and load, the dissipated heat energy is concentrated on water cooling and at higher engine speed and load, the output gas energy was higher than the water-cooling energy, not only in amount but also in exergy and percentages. Exergy efficiency is also higher.

At higher engine speeds and loads, exergy efficiency of the outlet gas is observed, while at lower engine speeds and loads, exergy efficiency of cooling water is observed. Theoretically, the fuel efficiency of this gasoline engine can be improved by recovering the heat dissipation and overall fuel efficiency up to 60%.

Dai et al. [28] proposed a new power and refrigeration hybrid cycle that combines the Rankine cycle and the ejector refrigeration cycle. The turbine cycle produces both power and cold at the same time. The system can operate with gas engine or gas turbine flue gas and also solar energy, geothermal energy and industrial waste heat. Exergy analysis is performed to improve the thermodynamics of this cycle and sensitivity analysis is performed to evaluate the effects of key thermodynamic parameters that affect the performance of the combined cycle. In addition, parametric optimization is performed using genetic algorithm to obtain the highest exergy efficiency. The results show that more exergy loss occurs due to irreversibilities in the additional heating process and the ejector causes more energy loss. It was also found that the turbine inlet pressure, turbine back pressure, condenser temperature and evaporator had a significant effect on the turbine output power, refrigeration output and exergy

efficiency of the combined cycle. The optimized exergy efficiency under these conditions is 27.1%.

Ramanathan and Gunasekaran [29] have simulated the vehicle ventilation system based on the absorption refrigeration cycle. The dissipative heat of the system acts as the absorption cooling actuator. The performance analysis of the steam absorption refrigeration system has been performed by developing a stable simulation model to find the limitations of the proposed system. The fluid is a mixture of water and lithium bromide which is selected due to its good thermodynamic and transfer properties compared to conventional refrigerants. The pump required for the proposed absorption refrigeration system is less than the power required for compressor operation. The condensing refrigeration system is common.

Evaluation of different energy recovery methods from vehicle thermal losses in actual operating conditions has not been considered in previous studies. In this paper, the energy recovery of a diesel car using three absorption, ejector and ORC is investigated for defined driving conditions.

II. PROBLEM DEFINITION

In this study, a specific diesel engine is considered and due to the thermal losses of this engine under different driving conditions, three systems are designed to recover energy losses for the purpose of generating power or cooling. These three systems comprise an ORC and two absorption and ejector refrigeration systems that have been investigated for different temperatures. These surveys for both urban and suburban driving are based on a specific program described below.

Table I outlines two plans for driving cars in the city and on the road. In urban traffic, there is a 10-minute drive at a speed of 20 km/h, 30 minutes at a speed of 40 km/h, 10 minutes at a speed of 60 km/h and 10 minutes at a speed of 80 km/h. In the second program, which is a 1-hour timetable on the road, 5 minutes' drive at 60 km/h, 10 minutes at 80 km/h, 25 minutes at 100 km/h and 20 minutes at 120 km/h are considered.

TABLE I
TWO PLANS FOR MOVING CARS IN THE CITY AND ON THE ROAD

Speed (km/h)	City Driving Time (min)	Road Driving Time (min)
20.0	10.0	0.0
40.0	30.0	0.0
60.0	10.0	5.0
80.0	10.0	10.0
100.0	0.0	25.0
120.0	0.0	20.0

III. PROBLEM THEORY

A. ORC

The ideal Rankin cycle is shown in Fig. 1. The cycle consists of four processes in the following order:

- Process 1 ⟶ 2: Increased reversible adiabatic pressure at the pump
- Process 2 ⟶ 3: Heating at constant pressure in the boiler

- Process 3 ⟶ 4: Reversible adiabatic expansion in the turbine
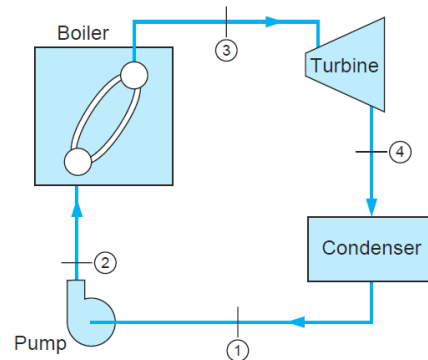- Process 4 ⟶ 1: Heat at constant pressure in condenser

Fig. 1 The ideal Rankine cycle [30]

The ORC structure is similar to the steam Rankine cycle and differs in the refrigerant that can recover heat from low temperature resources [31], [32]. Consequently, the performance of an ORC is as follows:

a. Evaporation, extraction of heat provided by the hot source
b. Expansion, output power generating
c. Distillation, unused residual heat discharge
d. Increase fluid pressure by pump

Based on their heat and temperature sources, operating fluid and its corresponding operating conditions have a serious impact on the cycle. Operating fluid can be classified according to the vapor saturation curve, which is one of the most important characteristics of operating fluid in the ORC. There are generally three types of saturation vapor curves in the temperature-entropy diagram (Fig. 2):

1- Dry fluid with positive slope,
2- Wet fluid with negative slope,
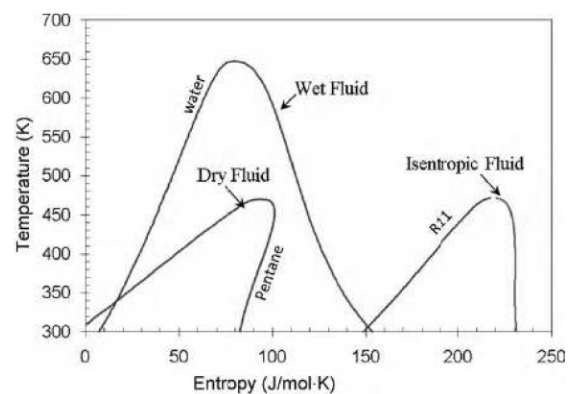3- Isentropic fluid with infinite slope.

Fig. 2 Temperature – entropy diagram for three types of fluid [33]

Water is a wet fluid that needs to be steam above the turbine inlet to prevent corrosion of the turbine blades. However, this is not the case for dry and isentropic fluids.

The thermal efficiency of the cycle is also obtained from the

following interface:

$$\eta_{th} = \frac{w_{net}}{q_H} = \frac{w_t - w_p}{q_H} \qquad (1)$$

Also, according to the first law of thermodynamics, for Rankine cycle we will have:

$$q_H - q_L = w_t - w_p \qquad (2)$$

By combining (1) and (2), the Rankin cycle thermal efficiency will be:

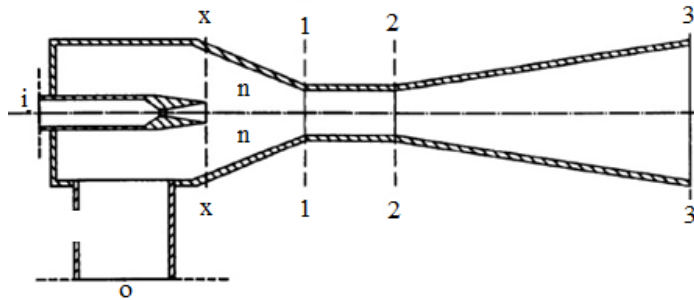$$\eta_{th} = \frac{q_H - q_L}{q_H} - = 1 - \frac{q_L}{q_H} \qquad (3)$$

B. Ejector Refrigeration

Fig. 3 shows an ejector refrigeration system.

Fig. 3 Ejector Refrigeration Cycle

Fig. 4 Different sections of a regular ejector

The performance of an ejector is defined as the ratio of absorption or mass flow ratio, which is the ratio between the rate of secondary and primary fluid mass flow:

$$\omega = \frac{m_s}{m_p} \qquad (4)$$

The performance of the ejectors can be evaluated using one-dimensional compressible flow theory. The initial model presented for the analysis of the air ejector was a one-dimensional model based on the ideal gas dynamics in terms of mass, momentum, and energy conservation concepts. The governing equations are presented below. The analysis is based on steady state and steady state for energy, momentum and continuum equations. The energy survival equation for the one-dimensional adiabatic process between input and output is as follows:

$$\sum m_i \left(h_i + \frac{v_i^2}{2} \right) = \sum m_e \left(h_e + \frac{v_e^2}{2} \right) \qquad (5)$$

Momentum equation:

$$P_i A_i + \sum m_i v_i = P_e A_e + \sum m_e v_e \qquad (6)$$

Continuity equation:

$$\sum \rho_i v_i A_i = \sum \rho_e v_e A_e \qquad (7)$$

where m, mass flow, h is the specific enthalpy, v velocity, P pressure, ρ density and A surface. According to Fig. 4, the following assumptions are applied for one-dimensional analysis:

1- Steam acts as a complete gas.
2- The ejector walls are insulated.
3- Frictional loss is introduced by applying isentropic efficiency for the primary nozzle, diffuser and mixing chamber.
4- Primary and secondary fluids are provided at zero velocity in sections i and o. The speed at the diffuser output 3-3 is assumed to be 0.
5- In Section 1-1 where the two primary flows overlap, static pressure is assumed to be uniform.
6- The mixing of two streams is completed before the normal suspense occurs at the end of the mixing chamber 3-3. The primary and secondary flow temperatures and the diffuser output flow are assumed to be stationary. Using the energy equation between ejector input and output, we have:

$$\dot{m}_p h_i + \dot{m}_s h_o = (\dot{m}_p + \dot{m}_s) h_3 \qquad (8)$$

Specific enthalpy is defined as follows:

$$h = c_{PV} T \qquad (9)$$

where c_{PV} is the specific heat at constant pressure and T is the absolute temperature. We have the combination of (7)-(9) and their rearrangement:

$$T_i + \omega T_o = (1 + \omega)T_3 \qquad (10)$$

The high pressure primary flow enters the primary nozzle and expands into the outlet (x-x plate) at low pressure. The high-speed primary flow enters the mixing chamber following the secondary fluid. During this process, the initial nozzle friction loss is considered by applying isentropic efficiency (η_p) to the equation. By applying the energy equation between i-x and o-x to the primary and secondary flows:

$$\dot{m}_p h_p = \dot{m}_{px}(h_{px} + \eta_p v_{px}^2/2) \qquad (11)$$

$$\dot{m}_s h_s = \dot{m}_{sx}(h_{sx} + v_{sx}^2/2) \qquad (12)$$

The input mass flow rate $\dot{m}_p$ m and the output mass rate m_{px} of the primary nozzle remain the same, giving the primary and secondary flow rates in the x-x region:

$$v_{px} = \sqrt{2\eta_p(h_p - h_{px})} \qquad (13)$$

$$v_{sx} = \sqrt{2(h_s - h_{sx})} \qquad (14)$$

Specific heat at constant pressure is defined as follows:

$$c_{PV} = \frac{kR}{k-1} \qquad (15)$$

where R is the ideal gas constant and k isentropic index of density and expansion.

The isentropic relationship between pressure and temperature ratios in states 1 and 2 is defined as:

$$\frac{T_1}{T_2} = \left(\frac{P_1}{P_2}\right)^{\frac{k-1}{k}} \qquad (16)$$

Sound speed at local static temperature is:

$$c = \sqrt{kRT} \qquad (17)$$

The local Mach number is defined as follows:

$$M = \frac{v}{c} \qquad (18)$$

The relationship between the pressure ratio along the nozzle and the Mach number at the nozzle output is:

$$M_{px} = \sqrt{\frac{2\eta_p}{(k-1)}\left(\left(\frac{P_i}{P_x}\right)^{\frac{k-1}{k}} - 1\right)} \qquad (19)$$

Similarly, for the primary nozzle, the secondary Mach number on the nozzle output plate will be:

$$M_{sx} = \sqrt{\frac{2}{(k-1)}\left(\left(\frac{P_o}{P_x}\right)^{\frac{k-1}{k}} - 1\right)} \qquad (20)$$

Mixing Process (Between Section n and Section 2)

By applying the momentum equation with the ideal mixing without loss between the initial nozzle at the output plate (section n) and at the output of the mixing chamber (section 2)

$$P_n A_n + \dot{m}_p v_{px} + \dot{m}_s v_{sx} = P_2 A_2 + (m_p + m_s)v_2 \qquad (21)$$

Assuming $P_n = P_2$ and $A_n = A_2$ we will have:

$$\dot{m}_p v_{px} + \dot{m}_s v_{sx} = (\dot{m}_p + \dot{m}_s)v_1 \qquad (22)$$

This relationship fully describes the ideal mixing process. By adding η_m as the total efficiency of the combustion chamber, the relationship will be more realistic as follows:

$$\eta_m(\dot{m}_p v_{px} + \dot{m}_s v_{sx}) = (\dot{m}_p + \dot{m}_s)v_1 \qquad (23)$$

Consequently, the combined fluid velocity in Section 1-1 is expressed as:

$$v_1 = \eta_m\left(\frac{\dot{m}_p v_{px} + \dot{m}_s v_{sx}}{\dot{m}_p + \dot{m}_s}\right) = \eta_m\left(\frac{v_{px} + v_{sx}}{1 + \omega}\right) \qquad (24)$$

Equation (24) can be written in relation to Mach number:

$$M_1^* = \frac{\eta_m(M_{px}^* + \omega M_{sx}^*\sqrt{\tau})}{\sqrt{(1 + \omega\tau)(1 + \omega)}} \qquad (25)$$

which is the ratio of the inertia temperatures to:

$$\tau = \frac{\tau_0}{\tau_i} \qquad (26)$$

The relationship between M and M* is as follows:

$$M^* = \frac{\sqrt{(k+1)M^2/2}}{\sqrt{1 + (k11)M^2/2}} \qquad (27)$$

Complex Flow after Shock Wave

At a certain distance in the combustion chamber, a transverse shock wave is induced which produces a compressive effect. Along this point, the speed of the mixed flow drops suddenly to the speed of sound. The complex Mach number after the shock wave is obtained from:

$$M_2 = \frac{M_1^2 + 2/(k-1)}{\left[\frac{2k}{k-1}\right]M_1^2 - 1} \qquad (28)$$

The pressure lift rate along the wave of doubt is also obtained from the following relation:

$$\frac{P_1}{P_2} = \frac{1 + kM_2^2}{1 + kM_1^2} \qquad (29)$$

Lift Pressure Rate along the Infrared Diffuser

The higher density of the mixed fluid is obtained when

passing through the infrared diffuser. The flow rate at the end of the diffuser (Section 3-3) is assumed to be zero. The pressure lift rate along the diffuser is obtained from:

$$\frac{P_3}{P_2} = \left[\frac{(k-1)\eta_d M_2^2}{2} + 1\right]^{\frac{k-1}{k}} \tag{30}$$

The critical pressure lift rate is also obtained from:

$$\frac{P_3}{P_o} = \left(\frac{P_3}{P_2}\right)\left(\frac{P_2}{P_x}\right)\left(\frac{P_x}{P_o}\right) = N_s^* \tag{31}$$

C. Absorption Refrigeration

The operating fluid in the absorption refrigeration system is a dual solution containing refrigerant and adsorbent. Fig. 5 shows the two vacuum ducts are connected to each other. The left duct contains liquid refrigerant and the right duct contains dual adsorbent and refrigerant solution. The right duct solution absorbs the refrigerant steam from the left duct and reduces pressure. When the refrigerant vapor is absorbed, the residual refrigerant temperature decreases due to evaporation. This results in the refrigeration effect occurring in the left duct. At the same time, the right duct solution becomes thinner as the absorbed refrigerant volume increases. This is called the absorption process. Naturally, the adsorption process is thermogenic, so it must give heat to the environment in order to maintain its absorption capacity. Whenever the solution cannot continue the adsorption process because the refrigerant becomes saturated, the refrigerant must be separated from the diluted solution. The refrigerant steam is distilled to the environment with the heat transferred. With these processes, the effect of refrigeration can be produced using thermal energy. However, the cooling effect cannot be produced continuously because the process cannot run simultaneously. As a result, the absorption refrigeration cycle is a combination of these two processes as shown in Fig. 6. When the separation process occurs at higher pressures than the adsorption process, a circulating pump is required for circulating the solution. The coefficient of performance of the absorption refrigeration system is obtained from:

$$COP = \frac{Produced\ Cooling\ in\ Evaporator}{Generator\ Heat\ Input + Pump\ Work} \tag{32}$$

The input work for the pump is neglected compared to the input heat in the generator, so pump work is often overlooked in the analyzes.
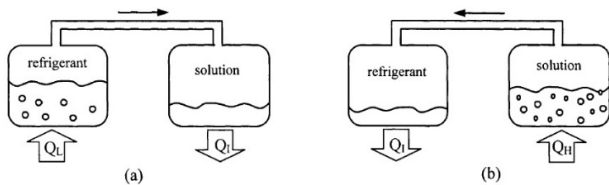

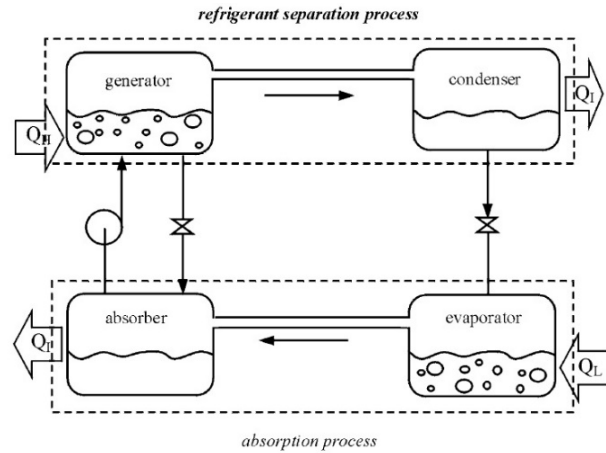Fig. 5 Adsorption Process in Absorption Refrigeration System [33]

Fig. 6 Absorption refrigeration cycle consisting of two adsorption processes [33]

IV. RESULTS

Further studies on energy recovery through the ORC, ejector refrigeration and absorption are presented below.

The diesel car with automatic transmission is desired and the recoverable thermal power at various speeds is shown in Fig. 7. As it is evident, with the increase in vehicle speed and power consumption, there is potential for more energy recovery.
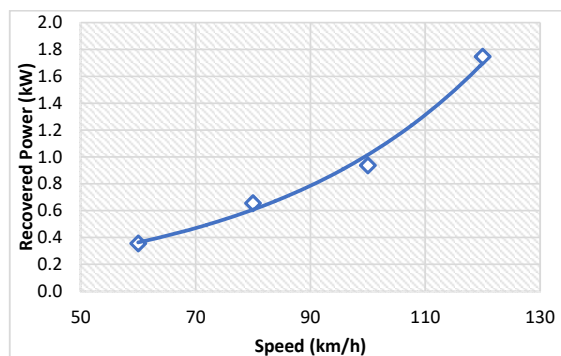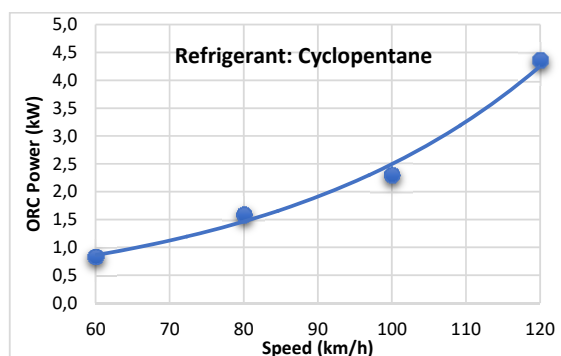

Fig. 7 Energy recovered at different speeds

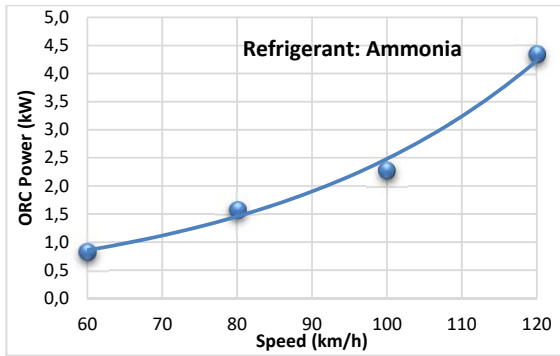Fig. 8 Extra power output at different vehicle speeds for Cyclopentane refrigerant

Fig. 9 Ammonia Refrigerant Generation of Extra Power at Different Vehicle Speeds
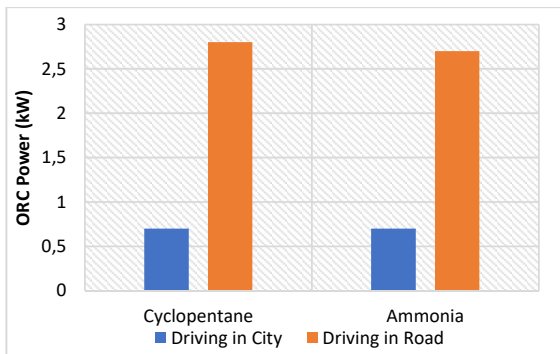

Fig. 10 Extra power output in two driving modes for different refrigerants

The amount of surplus power generated through the organic Rankine system using cyclopentane refrigerant at different speeds is shown in Fig. 8. Also, the amount of surplus power generated through the organic Rankine system using ammonia refrigerant is shown at different speeds in Fig. 9.

For the two driving programs considered, the amount of additional power generated by the proposed system is presented for different modes. The highest production capacity is related to cyclopentane, which is illustrated in Fig. 10 for urban and suburban driving.

Various refrigerants can be used to recover energy from vehicle heat losses through an ejector system, some of which are examined.
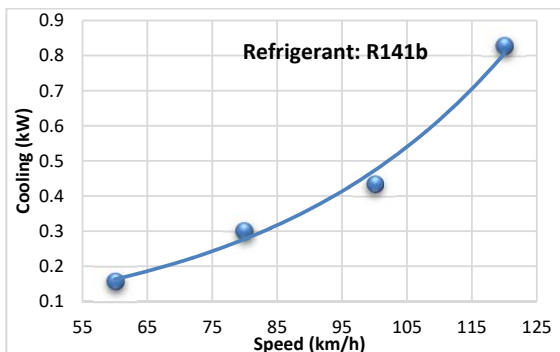

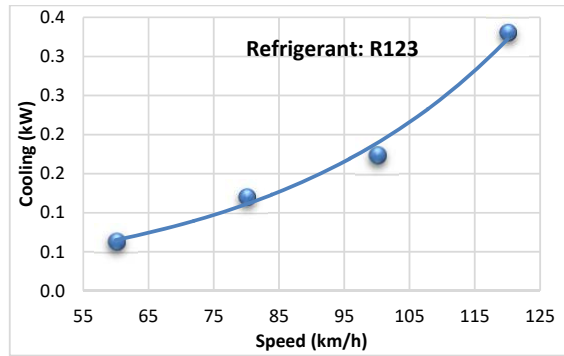Fig. 11 The amount of cooling power produced by R141b

Fig. 12 The amount of cooling power produced by R123

The amount of cooling power generated by the ejector hybrid system using R141b refrigerant at different speeds is shown in Fig. 11.

The amount of cooling power generated by the ejector hybrid system using R123 refrigerant at different speeds is shown in Fig. 12. Also, the amount of cooling power output through the ejector hybrid system using R134a refrigerant at different speeds is shown in Fig. 13.

For the two considered driving plans, produced cooling for different refrigerants is provided. The highest cooling production is related to R141b, which is illustrated in Table II for urban and suburban driving.
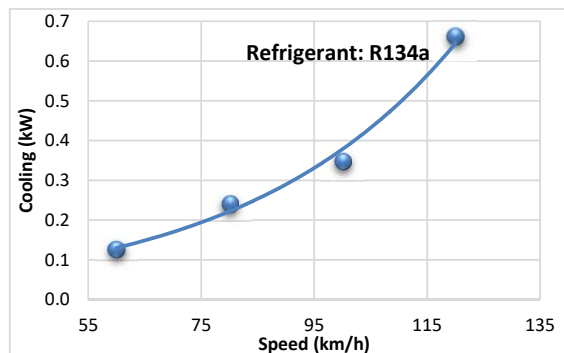

Fig. 13 The amount of cooling power generated by R134a

TABLE II
COOLING RATES WITH DIFFERENT REFRIGERANTS FOR CITY AND ROAD DRIVING MODES

Refrigerant	Cooling Produced in City Driving (kWh)	Cooling Produced in Road Driving (kWh)
R141b	1.3	5.2
R123	0.5	2.1
R134a	1	4.2

Fig. 14 shows the amount of cooling power generated by the absorption hybrid system at different ambient temperatures.

For the two driving plans, the amount of generated cooling at different ambient temperatures is shown in Fig. 15. When the ambient temperature is lower, the amount of cooling produced is higher due to the better efficiency of the cooling system and also, we see better results in the road driving type.
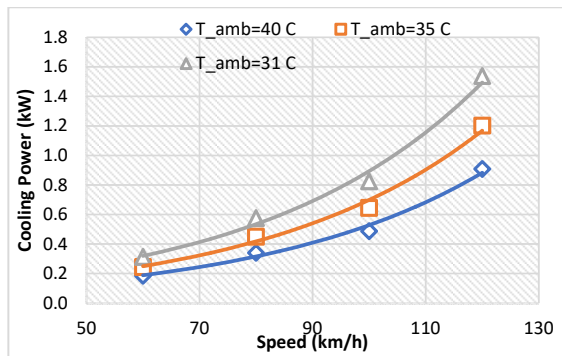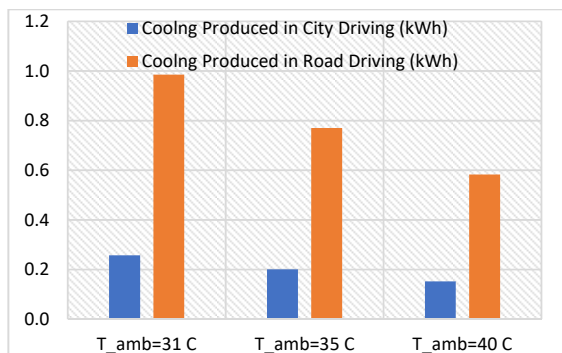
Fig. 14 Cooling Power Generation

Fig. 15 Cooling rate for urban and road driving at different ambient temperature conditions

V. CONCLUSION

Using three systems of organic Rankine auxiliary power generation, ejector and also absorption refrigeration were analyzed to recover energy from a diesel car. The highest power generation through the ORC system was achieved at 0.7 kWh for city driving and 2.8 kWh for road driving with refrigerant cyclopentane, respectively. Also, the cooling produced in the absorption refrigeration system in the urban and suburban states is 2.6 and 9.9 kWh, and in the ejector refrigeration system 1.3 and 5.2 kWh for refrigerant R141b.

REFERENCES

[1] Xu, F., Goswami, D.Y., Bhagwat, S.S., "A combined power/ cooling cycle", Energy, 25, 233–246, 2000.
[2] A. A. Hasan, D. Y. Goswami, and S. Vijayaraghavan, "First and second law analysis of a new power and refrigeration thermodynamic cycle using a solar heat source," *Solar Energy,* vol. 73, pp. 385-393, 2002.
[3] G. Tamm, D. Goswami, S. Lu, and A. Hasan, "Theoretical and experimental investigation of an ammonia–water power and refrigeration thermodynamic cycle ",*Solar Energy,* vol. 76, pp. 217-228, 2004.
[4] A. Vidal, R. Best, R. Rivero, and J. Cervantes, "Analysis of a combined power and refrigeration cycle by the exergy method," *Energy,* vol. 31, pp. 3401-3414, 2006.
[5] S. Vijayaraghavan and D. Goswami, "A combined power and cooling cycle modified to improve resource utilization efficiency using a distillation stage," *Energy,* vol. 31, pp. 1177-1196, 2006.
[6] C. Martin and D. Goswami, "Effectiveness of cooling production with a combined power and cooling thermodynamic cycle," *Applied Thermal Engineering,* vol. 26, pp. 576-582, 2006.
[7] S. Sadrameli and D. Goswami, "Optimum operating conditions for a combined power and cooling thermodynamic cycle," *Applied Energy,* vol. 84, pp. 254-265, 2007.
[8] D. Zheng, B. Chen, Y. Qi, and H. Jin, "Thermodynamic analysis of a novel absorption power/cooling combined-cycle," *Applied Energy,* vol. 83, pp. 311-323, 2006.
[9] M. Liu and N. Zhang, "Proposal and analysis of a novel ammonia–water cycle for power and refrigeration cogeneration," *Energy,* vol. 32, pp. 961-970, 2007.
[10] N. Zhang and N. Lior, "Methodology for thermal design of novel combined refrigeration/power binary fluid systems," *International Journal of Refrigeration,* vol. 30, pp. 1072-1085, 2007.
[11] N. Zhang and N. Lior, "Development of a novel combined absorption cycle for power generation and refrigeration," *Journal of Energy Resources Technology,* vol. 129, pp. 254-265, 2007.
[12] J. Wang, Y. Dai, and L. Gao, "Parametric analysis and optimization for a combined power and refrigeration cycle," *Applied energy,* vol. 85, pp. 1071-1085, 2008.
[13] M. Ameri, A. Behbahaninia, and A. A. Tanha, "Thermodynamic analysis of a tri-generation system based on micro-gas turbine with a steam ejector refrigeration system," *Energy,* vol. 35, pp. 2203-2209, 2010/05/01/ 2010.
[14] J. Wang, Y. Dai, and Z. Sun, "A theoretical study on a novel combined power and ejector refrigeration cycle," *International Journal of Refrigeration,* vol. 32, pp. 1186-1194, 2009/09/01/ 2009.
[15] R. Yapıcı, "Experimental investigation of performance of vapor ejector refrigeration system using refrigerant R123," *Energy Conversion and Management,* vol. 49, pp. 953-961, 2008/05/01/ 2008.
[16] R. Yapıcı and C. C. Yetişen, "Experimental study on ejector refrigeration system powered by low grade heat," *Energy Conversion and Management,* vol. 48, pp. 1560-1568, 2007/05/01/ 2007.
[17] T. Sankarlal and A. Mani, "Experimental investigations on ejector refrigeration system with ammonia," *Renewable Energy,* vol. 32, pp.2007 /01/07/2007 ,1413-1403
[18] K. Pianthong, W. Seehanam, M. Behnia, T. Sriveerakul, and S. Aphornratana, "Investigation and improvement of ejector refrigeration system using computational fluid dynamics technique," *Energy Conversion and Management,* vol. 48, pp. 2556-2564, 2007/09/01/ 2007.
[19] H. Golchoobian, M. Amidpour, and O. Pourali, "Thermodynamic analysis of three combined power and refrigeration Systems based on a demand," *Gas Processing,* vol. 6, pp. 29-40, 2018.
[20] H. Golchoobian, A. Behbahaninia, M. Amidpour, and O. Pourali, "Dynamic Exergy Analysis of a Solar Ejector Refrigeration System with Hot Water Storage Tank," in *Progress in Sustainable Energy Technologies: Generating Renewable Energy,* I. Dincer, A. Midilli, and H. Kucuk, Eds., ed Cham: Springer International Publishing, 2014, pp. 327-337.
[21] C. Yue and P. Wang, "Thermal analysis on vehicle energy supplying system based on waste heat recovery ORC," *Energy Procedia,* vol. 158, pp. 5587-5595, 2019.
[22] S. G. Herawan, K. Talib, and A. Putra, "Prediction of heat energy from the naturally aspirated internal combustion engine exhaust gas using artificial neural network," *Procedia Computer Science,* vol. 135, pp. 267-274, 2018.
[23] B. Mashadi, A. Kakaee, and A. J. Horestani, "Low-temperature Rankine cycle to increase waste heat recovery from the internal combustion engine cooling system," *Energy Conversion and Management,* vol. 182, pp. 451-460, 2019.
[24] B. Patel, N. B. Desai, and S. S. Kachhwaha, "Optimization of waste heat based organic Rankine cycle powered cascaded vapor compression-absorption refrigeration system," *Energy conversion and management,* vol. 154, pp. 576-590, 2017.
[25] C. Yue, L. Tong, and S. Zhang, "Thermal and economic analysis on vehicle energy supplying system based on waste heat recovery organic Rankine cycle," *Applied Energy,* vol. 248, pp. 241-255, 2019.
[26] F. Salek, A. N. Moghaddam, and M. M. Naserian, "Thermodynamic analysis of diesel engine coupled with ORC and absorption refrigeration cycle," *Energy Conversion and Management,* vol. 140, pp. 240-246, 2017.
[27] J. Fu, J. Liu, R. Feng, Y. Yang, L. Wang, and Y. Wang, "Energy and exergy analysis on gasoline engine based on mapping characteristics experiment," *Applied Energy,* vol. 102, pp. 622-630, 2013.
[28] Y. Dai, J. Wang, and L. Gao, "Exergy analysis, parametric analysis and optimization for a novel combined power and ejector refrigeration cycle," *applied thermal engineering,* vol. 29, pp. 1983-1990, 2009.
[29] A. Ramanathan and P. Gunasekaran, "Simulation of Absorption

Refrigeration System for Automobile Application," *Thermal Science,* vol. 12, pp. 5-13, 2008.

[30] R. E. Sonntag, C. Borgnakke, G. J. Van Wylen, and S. Van Wyk, *Fundamentals of thermodynamics* vol. 6: Wiley New York, 1998.

[31] S. Quoilin, M. Van Den Broek, S. Declaye, P. Dewallef, and V. Lemort, "Techno-economic survey of Organic Rankine Cycle (ORC) systems," *Renewable and Sustainable Energy Reviews,* vol. 22, pp. 168-186, 2013.

[32] T.-C. Hung, T. Shai, and S. K. Wang, "A review of organic Rankine cycles (ORCs) for the recovery of low-grade waste heat," *Energy,* vol. 22, pp. 661-667, 1997.

[33] P. Srikhirin, S. Aphornratana, and S. Chungpaibulpatana, "A review of absorption refrigeration technologies," *Renewable and sustainable energy reviews,* vol. 5, pp. 343-372, 2001.